3. METHODOLOGY

Equation (3.2.3) above is premised on the assumption that the distribution of electrons in the sample is confined to spherically symmetric atoms, *i.e.,* ignoring charge density in bonds and the deformation of core electron density. For the purposes of phase identification and structure refinement, this is generally a good approximation. X-ray determination of non-spherical charge densities goes beyond the scope of this introduction; for further information, see *e.g.* Coppens (1997) and Bindzus *et al.* (2014).

In energy-dispersive X-ray measurements, the detector sits at a fixed 2θ and collects diffracted radiation from a continuum source. The independent variable of the measurement can be taken as the X-ray energy, $E = hc/\lambda$. With the appropriate change of variables, equation (3.2.2) can be written as

$$\frac{d\sigma}{d\Omega} = \frac{Nr_e^2}{16\pi V}\frac{h^3c^3Pm_{hkl}}{E^2\sin^3\theta}|A_{hkl}|^2\delta\left(E - \frac{hc}{2d\sin\theta}\right). \qquad (3.2.7)$$

Recall that $hc = 12.398$ KeV Å in convenient units. Again, instrument resolution and sample effects will broaden the peak, but its integrated area is given by the terms preceding the delta-function. Of course, the diffracted intensity must be normalized to the incident spectrum as a function of energy; this may be a rather complicated undertaking as it involves energy-dependent corrections for such factors as detector sensitivity, absorption in the sample *etc.*

3.2.2.2.2. *Neutrons and nuclear scattering*

Neutrons interact with the sample in two ways: the strong interaction with the atomic nuclei, and the magnetic interaction between the neutron's dipole moment and magnetization density in the sample. We consider here only unpolarized neutrons; the use of polarized neutrons permits separation between nuclear and magnetic scattering as well as direct observation of the interference between the two; details are beyond the scope of this chapter. Nuclear scattering is very similar to the X-ray case discussed above, except that the atomic scattering amplitude $r_e f_n$ is replaced by the nuclear coherent scattering length $\bar{b}_n$ (given in *International Tables for Crystallography*, Volume C, Table 4.4.4.1), which is generally independent of neutron energy.

Unlike X-rays, the strength of the neutron–nucleus interaction is not a smooth function of atomic number. This creates opportunities to use neutrons to distinguish atoms with nearly identical X-ray scattering amplitudes, but it also makes certain elements very difficult to study with neutrons. The interaction between neutrons and the nuclei in the sample depends on the isotope and possibly the spin angular momentum of the neutron–nucleus system. This means that incoherent scattering can be significantly larger than the (coherent) diffracted signal for certain atoms, notably hydrogen (^{1}H); see Chapter 2.3 of this volume for further details. For wavelengths of interest in crystallography, the nucleus is essentially a point, and so there is no atomic form factor. This generally leads to greater intensity relative to X-rays at increasing scattering vector (decreasing d-spacing).

Neutron diffractometers operate in one of two ways: angle dispersive or energy dispersive. The configuration for angle-dispersive diffraction measurements is conceptually similar to that used for X-rays; a monochromatic beam of neutrons impinges on the sample and a detector measures the distribution of neutrons *versus* scattering angle. For Bragg neutron diffraction from nuclei,

$$\frac{d\sigma}{d\Omega} = \frac{N\lambda^3}{16\pi V}\frac{m_{hkl}}{\sin\theta\sin 2\theta}|A_{hkl}^{(n)}|^2\delta\left(2\theta - 2\sin^{-1}\frac{\lambda}{2d}\right), \qquad (3.2.8)$$

where the neutron nuclear structure factor is defined as

$$A_{hkl}^{(n)} = \sum_n \bar{b}_n \exp(2\pi i\mathbf{G}\cdot\mathbf{r}_n)\exp(-W). \qquad (3.2.9)$$

Time-of-flight neutron diffractometers, generally based at pulsed spallation sources, operate by measuring the time from the creation of the pulse of neutrons at the target until they appear in a given detector. If the total path length from source to detector is L and the detector is situated at an angle 2θ, a neutron with time of flight t had speed L/t and wavelength $\lambda = ht/m_nL$. Here h is Planck's constant and m_n is the mass of the neutron. This provides a measurement of the d-spacing within the sample, $d = ht/(2m_nL\sin\theta)$. Another change of variables from equation (3.2.2) yields

$$\frac{d\sigma}{d\Omega} = \frac{N}{64\pi V}\left(\frac{h}{m_nL}\right)^3\frac{t^4}{\sin^2\theta}m_{hkl}|A_{hkl}|^2\delta(t - 2d\sin\theta Lm_n/h). \qquad (3.2.10)$$

In practice, a large number of detectors surround the sample and counts from the same d-spacing (appropriately normalized for incident-beam intensity and detector solid angle) are binned together. In convenient units, $m_n/h = 253$ μs m^{-1} Å^{-1}.

3.2.2.2.3. *Neutrons and magnetic scattering*

Magnetic neutron scattering is also described through a structure factor which is, however, a vector. The magnetic moment of the neutron interacts with the magnetization density of unpaired electrons in the sample, which may possess spin and/or orbital angular momentum. The magnetic interaction is only sensitive to the component of magnetization perpendicular to the scattering vector. When discussing magnetic scattering, it is more common to use the scattering vector $\mathbf{Q} = 2\pi\mathbf{G}$. The magnetic structure factor is defined as

$$\mathbf{A_Q}^{mag} = (\gamma r_e/2)\sum_n f_n(Q)(\hat{\mathbf{Q}}\times\mathbf{m}_n\times\hat{\mathbf{Q}})\exp(i\mathbf{Q}\cdot\mathbf{r_n})\exp(-W). \qquad (3.2.11)$$

Here $\gamma = 1.9132$ is the neutron gyromagnetic factor, $f_n(Q)$ is the atomic magnetic form factor, $\mathbf{m}_n$ is the magnetization of the nth site in units of the Bohr magneton and $\hat{\mathbf{Q}}$ is the unit vector in the direction of $\mathbf{Q}$. The double cross product isolates the component of magnetization perpendicular to $\mathbf{Q}$.

Note that many magnetically ordered materials have a magnetic cell which is larger than the chemical cell. Indeed, many magnetic phases are incommensurately modulated, *i.e.*, the magnetic structure is not periodic with any combination of the chemical unit cell translation vectors. Such matters are beyond the scope of this introduction, and are handled in Chapter 7.13 of this volume.

For unpolarized neutron measurements (*i.e.*, an average over all polarization states of the incoming and diffracted beam), the intensities of the nuclear and magnetic diffraction peaks may be computed separately and then added to determine the overall diffraction pattern. In cases where the chemical and magnetic cells are identical (*e.g.* simple ferromagnets) the nuclear and magnetic diffraction patterns overlap, and so one observes only intensity differences upon magnetic ordering. In the case of antiferromagnets, new magnetic diffraction peaks appear at positions not allowed for the chemical unit cell.

Note also that the magnetic form factor depends on the spin density in the magnetic orbitals, which are typically of greater spatial extent than either the total charge density or the nuclear

density. Therefore, the intensity of magnetic neutron diffraction peaks falls off much more rapidly with $(\sin\theta)/\lambda$ than do nuclear neutron diffraction peaks.

3.2.2.3. *Peak shapes*

The shape of a powder-diffraction peak is a convolution of the intrinsic line shape due to the microscopic structure of the sample crystallites (*e.g.* size and strain) and the configuration of the instrument used to record the pattern. A major goal of powder-diffraction analysis is to be able to separate the contributions of instrument and sample, so that information about the micro-structure of the sample can be extracted reliably. On the other hand, in some cases one simply wants to be able to model the combined influence of instrument and sample, to obtain a functional form that permits the most accurate way of apportioning intensities to partially overlapping peaks.

Consider first the sample-dependent factors. The following division into size and strain effects is somewhat artificial, insofar as lattice strains affect the size of the coherently diffracting domain. Nevertheless, it is common to make a distinction between the two, as size broadening produces a peak width proportional to $1/\cos\theta$ in angle-dispersive measurements, whereas the peak width is proportional to $\tan\theta$ for strain broadening.

3.2.2.3.1. *Domain size*

In very general terms, diffraction peaks from an object of linear size L will have a width in Q of the order of $1/L$. As formulated by Scherrer (1918), in an angle-dispersive measurement, the full width at half-maximum (FWHM) in 2θ, measured in radians, is given by

$$\Gamma = \frac{K\lambda}{L\cos\theta}, \qquad (3.2.12)$$

where K is called the shape factor and is a number of the order of unity whose precise value depends on the shape of the particles, which are assumed to be of uniform size and shape. The FWHM shape factor for a spherical particle is $K = 0.829$ (Patterson, 1939). Note that if a powder sample is polydisperse (*i.e.*, it contains a distribution of grain sizes), the average grain size is not necessarily given by the Scherrer equation.

Perhaps a more useful measure of the width of a peak is the integral breadth. In an angle-dispersive measurement, the integral breadth of a given peak centred at $2\theta_0$ is defined as

$$\beta = \frac{1}{I(2\theta_0)}\int I(2\theta)\,\mathrm{d}2\theta.$$

From a technical point of view, measurement of the integral breadth requires accurate measurement of the intensity in the wings of the diffraction peak, which in turn depends on accurate knowledge of the background intensity.

For any crystallite shape, it can be shown that the integral breadth is related to the volume-average thickness of the crystallite in the direction of the diffraction vector, *viz.*

$$L_V = \frac{\lambda}{\beta\cos\theta} = \frac{1}{V}\int \mathrm{d}^3\mathbf{r}\,T(\mathbf{r},\mathbf{G}),$$

where V is the volume of the crystallite and $T(\mathbf{r},\mathbf{G})$ is the length of the line inside the crystallite parallel to $\mathbf{G}$ and passing through the point $\mathbf{r}$. For example, if one writes an integral-breadth version of the Scherrer equation,
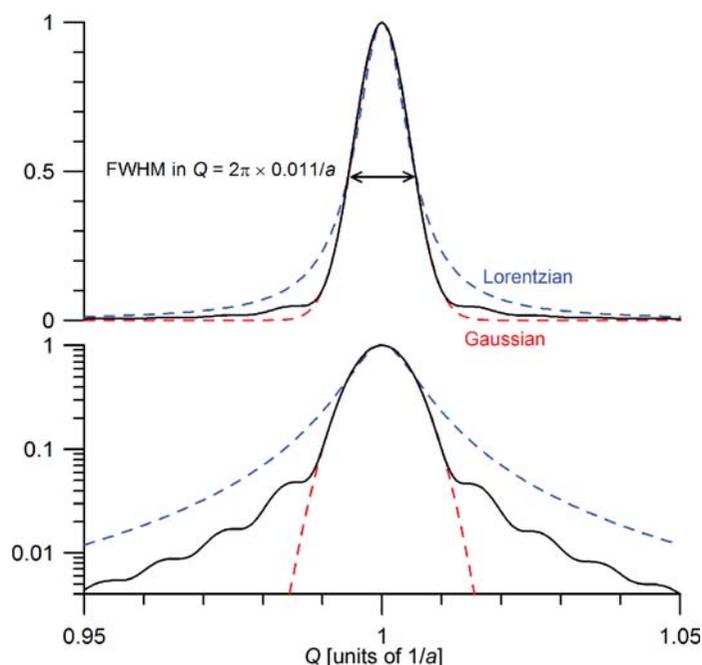

Figure 3.2.1
Computed powder line shape from an ensemble of spherical particles of diameter $100a$, including comparison to Gaussian and Lorentzian line shapes of equal FWHM.

$$\beta = \frac{K_\beta\lambda}{L\cos\theta},$$

the shape factor K_β is unity for $(00l)$ reflections from cube-shaped crystals of size L. $K_\beta = 1.075$ for a sphere of diameter L.

An important feature of the integral breadth is that it has a well defined meaning for a polydisperse sample of crystallites. Assuming that the crystallites all have the same shape,

$$\beta = \frac{K_\beta\lambda\langle L^3\rangle}{\cos\theta\langle L^4\rangle},$$

where $\langle L^3\rangle$ and $\langle L^4\rangle$ are the third and fourth moments of the size distribution (Langford & Wilson, 1978).

In many applications such as Rietveld or profile refinement, it is important to treat the full shape of the diffraction peak instead of merely its width (Loopstra & Rietveld, 1969; Rietveld, 1969). By way of illustration, Fig. 3.2.1 shows one Bragg peak of the computed powder-diffraction pattern from an ensemble of spherical particles of point scatterers in a simple cubic lattice. The lattice parameter is a, and the diameter of the particles is chosen to be $100a$, so that each crystallite consists of approximately 5.2×10^5 'atoms'. (This line shape was calculated using the Debye equation, described in Section 3.2.4.)

Several different analytical functions are frequently used in powder diffraction. In terms of the independent variable x, centred at x_0 with FWHM Γ, the normalized Gaussian function is

$$G(x-x_0) = \pi^{-1/2}\sigma^{-1}\exp-\left(\frac{x-x_0}{\sigma}\right)^2,$$

with $\sigma = \Gamma/2(\ln 2)^{1/2}$. The normalized Lorentzian is

$$L(x-x_0) = \frac{\Gamma/2\pi}{(x-x_0)^2 + (\Gamma/2)^2}.$$

The symmetric Pearson-VII function is a generalization of the Lorentzian, written as